CHAPTER III: METHODS OF ANALYSIS USING SAFIR FINITE ELEMENT COMPUTER CODE

III.1 Introduction to SAFIR

In this research, the computer program SAFIR is used to analyse the behaviour of composite columns under normal and fire conditions. SAFIR is a non-linear code developed at the University of Liege. It is especially devoted to the analysis of structures under elevated temperature conditions, although it can also be used to analyse structures under ambient conditions. The program, which is based on the Finite Element Method (FEM), can be used to study the behaviour of two and three-dimensional structures. SAFIR accommodates various elements for different idealizations, calculation procedures and material models incorporating stress-strain behaviour. The elements include 2-D SOLID, 3-D SOLID, BEAM, SHELL and TRUSS elements. The stress-strain material laws are generally linear-elliptic for steel and non-linear for concrete. Some predefined material models are embedded in the code, namely concrete, steel, wood, and aluminium materials.

Using the program, the analysis of a structures exposed to fire consists of two steps. The first step involves predicting the temperature distribution inside the structural members, referred to as "thermal analysis". The second step, named "structural analysis", is carried out in order to determine the mechanical response of the structure due to the thermal effects, since the load is usually assumed to remain constant during the fire.

A structure can of course be analysed at normal temperature up to failure, but in this case, the temperature dependent material properties are replaced by those at room temperature.

Detailed information about the code SAFIR is given by Franssen J.M. (1997, 2005), Nwosu D.I. *et al.* (1999). The validity of the code SAFIR has been demonstrated in various references such as: Franssen J.M. *et al.* (1994), Pintea D. & Franssen J.M. (1997), Kodur V.K.R *et al.* (1999b), Talamona D. *et al.* (2003). SAFIR has been used to study the behaviour of steel, concrete or composite structures (Franssen J.M. *et al.* (1993-2007), Dotreppe J.C. *et al.* (1999), Vila Real P.M.M. *et al.* (2003-2007), Lim L. *et al.* (2004), Njankouo J.M. *et al.* (2005), Talamona D. *et al.* (2005).

III.2 Thermal model of SAFIR applied to CFSHS columns

III.2.1 Thermal environment

In fact any fire curve can be used in the thermal model of SAFIR such as external fires, hydrocarbon curves and natural fires. In all examples analysed in this chapter, the ISO 834 fire has been applied.

The ISO 834 fire is defined according to the following equation:

$$T = 345.\lg(8t + 1) + T_0$$

where t is the time (minutes), T_0 is the ambient temperature (°C) and T is the temperature at time t

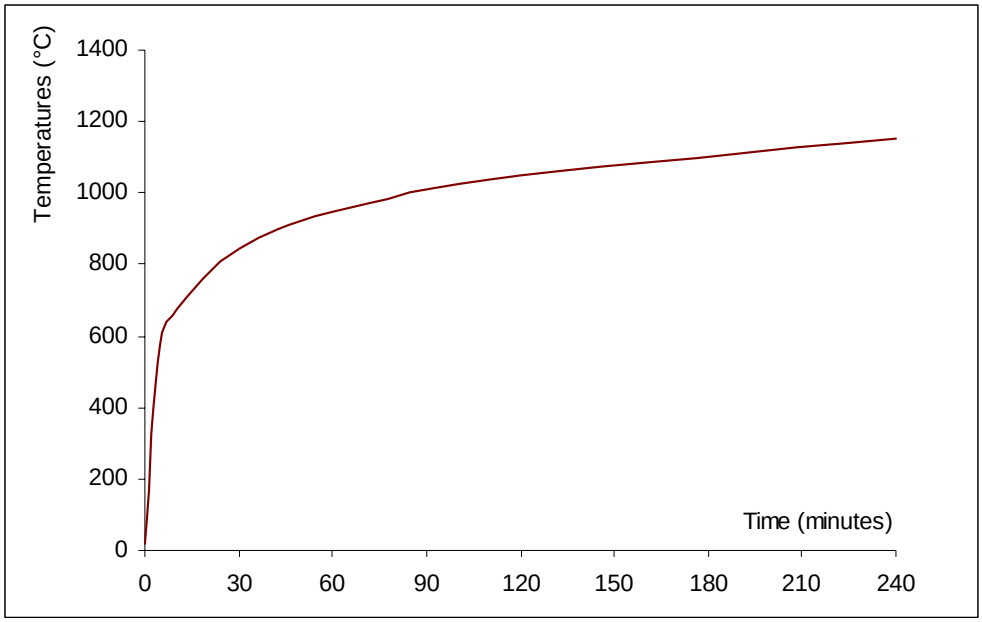

Figure III-1. Time-temperature curve ISO 834

III.2.2 Numerical approach for the thermal analysis

A uniform temperature is assumed over the height of the column. Thus, thermal analysis can be reduced to a two-dimensional problem of transient heating. The non-steady-state 2D temperature distribution within any cross-section is determined by the Fourier thermal conductivity equation:

$$k\left(\frac{\partial^2 T}{\partial x^2}+\frac{\partial^2 T}{\partial y^2}\right)+Q=\rho.c.\frac{\partial T}{\partial t}$$

where k is the thermal conductivity of the material, T is the temperature, Q is the amount of heat generated in the material per unit volume, ρ is the density, c is the heat capacity, t is the time and x, y are the position coordinates.

The temperature field within a given network is established by a finite element method in conjunction with an integration method for time steps. It is assumed that conduction is the main heat transfer mechanism in the hollow steel section and concrete core. Convection and radiation act essentially as heat transfer from the fire environment to the external hollow steel section. The influence of moisture (assumed uniformly distributed in the concrete) is treated in a simplified way: the transient temperatures in the concrete are calculated assuming that all moisture evaporates, without any transfer, at temperatures situated within a narrow range, with the heat of evaporation giving a corresponding change in the enthalpy-temperature curve. Therefore during the period of evaporation, all the heat supplied to an element is used for the moisture evaporation until the element is dry.

The discretization for plane sections of different shapes is possible by using triangular and/or quadrilateral elements. For each element the material can be defined separately. Any material can be analysed provided its physical properties at elevated temperatures are known. The variation of material properties with temperature can be considered.

In square or circular sections, there are two axes of symmetry, therefore only one quarter of

the section has to be discretized. Figure III-2 shows an example of such a discretization.

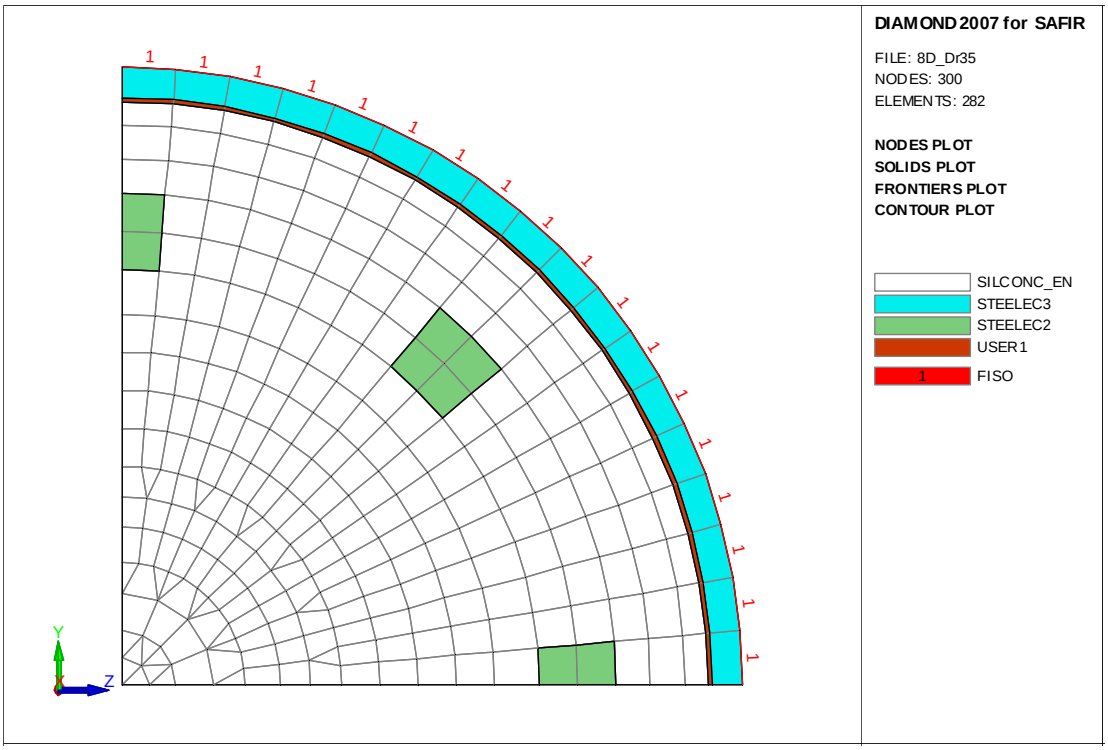

Figure III-2. Discretization of one-quarter of a square section

The cross- section is divided into elements with a size not exceeding 15 mm. A sensitivity study has been carried out to assess whether it is necessary to adopt elements with smaller size. A comparison of temperatures in reinforced steel and at some points in concrete in two meshing cases has been done: one case with the element dimension around 15 mm and one case with much smaller dimension (about 5mm). It can be seen that the temperatures do not differ much in the two cases (Figure III-3 and Figure III-4).

The meshing also affects the structural analysis because the same discretisation is used. The integration of the longitudinal stresses and stiffness on the section is based on the fibre model, each finite element of the thermal analysis, with its known material type and temperature, is considered as a fibre. So in most simulations, the cross-section is discretized with all element dimensions of around 10 mm.

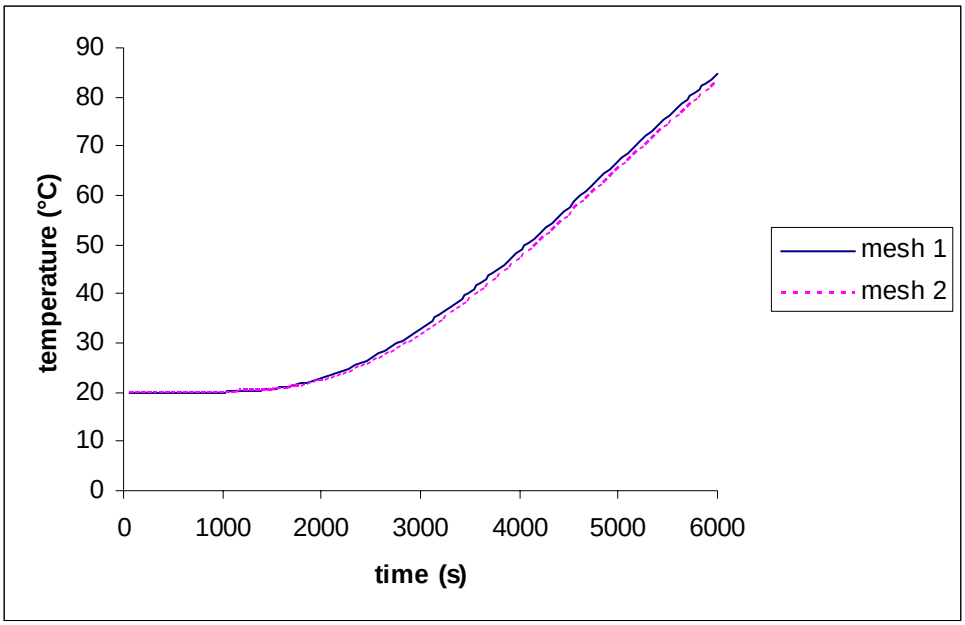

Figure III-3. Temperatures at one point in concrete

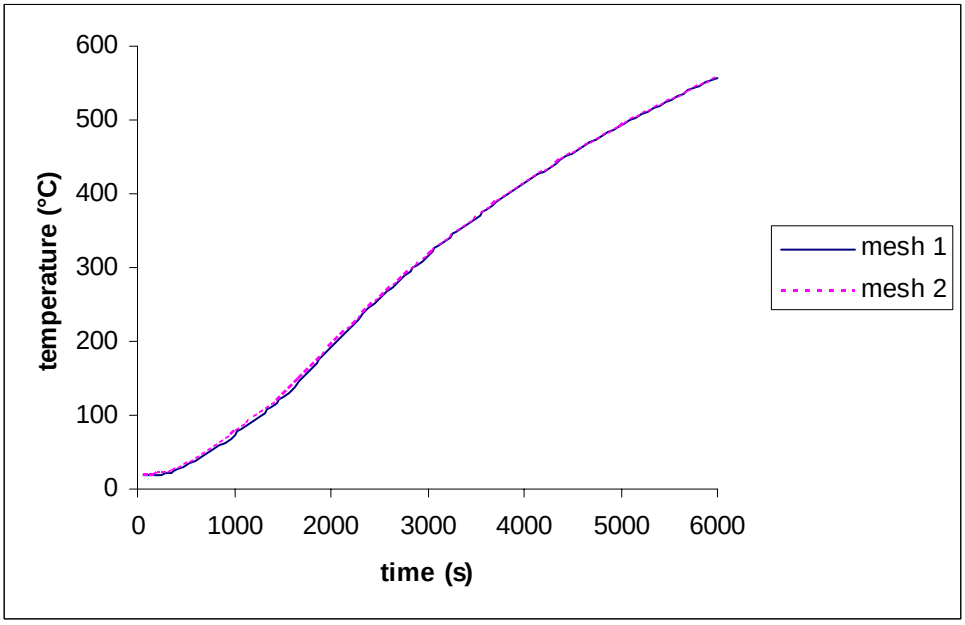

Figure III-4. Temperatures at the reinforcing bar

III.2.3 Main assumptions used in the numerical simulations

Using SAFIR programme, the simulations of the heating of CFSHS columns exposed to fire have been conducted using the following assumptions:

- The same water content 4% in weight is taken into account for all tests;
- The thermal properties (thermal conductivity, specific heat capacity) are those given by Eurocode 4 - EN1994-1-2. Siliceous concrete is considered. The upper limit of the thermal conductivity of concrete id used because this curve has been

derived from tests of steel-concrete composite structural elements (EN 1994-1-2). The detail can be found in Appendix 1;

- The gas temperature is assumed to rise according to standard time-temperature curve ISO 834;
- To calculate the heat flow transmitted to the surface of the hollow steel section during the fire exposure, it is necessary to introduce the value of the convection heat transfer (h_c) and the resultant emissivity (ε_m). In practice, whatever the nature of materials, the convection coefficient inside the furnaces is taken equal to $h_c = 25 \quad W/m^2K$. The resultant emissivity $\varepsilon_m = 0.7$ according to EN 1994-1-2;
- The thermal resistance at the steel-concrete interface is taken into account by simulating the thermal interaction (gap) between hollow steel section and concrete core. The thermal resistance R_c is assumed constant along the steel-concrete interface and independent of the temperature. The very thin layer of material "USER1" is used to take into account this thermal resistance. This layer has the following characteristics: thickness t = 0.001m, the conductivity $\lambda = t/R_c$. Other research works indicate that the value of R_c is closed to 0.010 m^2K/W (Renaud C. (2004)). Here the value R= 0.013 m^2K/W has been adopted. This value has been obtained by numerical experimentation in order to get a satisfactory correlation between numerical results and test results collected from other research studies.

III.2.4 Validity of the thermal model

Twenty seven fire tests carried out in Europe: University of Braunschweig–Germany (Kordina K. and Klingsch W. (1983)) and CTICM-France (Renaud C. (2004)), and in North America: National Research Council of Canada (Chabot M. and Lie T.T. (1992), Myllymaki J. et al (1994)) have been simulated. The main structural characteristics of the column tests are reported in Table III.1

Test Number	Section	Size (mm)	Thickness (mm)	Reinforcements	Concrete Cover (mm)	Reference	
						N°	Reference
1	Square	200	6.3	4Ø18	30	1/1	Kordina (1983)
2	Square	200	6.3	4Ø18	30	1/2	Kordina (1983)
3	Square	200	6.3	4Ø18	30	1/5	Kordina (1983)
4	Square	200	6.3	4Ø18	30	1/6	Kordina (1983)
5	Square	260	7.1	4Ø18	30	1/9	Kordina (1983)
6	Square	300	7.0	4Ø18	30	1/10	Kordina (1983)
7	Square	200	6.3	4Ø18	30	1/13	Kordina (1983)
8	Square	200	6.3	4Ø10	30	1/16	Kordina (1983)
9	Square	200	6.3	-	-	1/17	Kordina (1983)
10	Square	200	6.3	4Ø18	30	1/18	Kordina (1983)
11	Square	200	6.3	4Ø18	30	1/19	Kordina (1983)
12	Square	200	6.3	4Ø18	30	1/20	Kordina (1983)
13	Square	200	6.3	4Ø18	30	1/21	Kordina (1983)
14	Square	200	6.3	2(2Ø10+1Ø22)	30	1/22	Kordina (1983)
15	Square	220	6.3	4Ø18	30	1/23	Kordina (1983)
16	Square	220	6.3	6Ø20	30	1/24	Kordina (1983)
17	Square	260	7.1	6Ø22	30	1/25	Kordina (1983)
18	Square	300	7.0	6Ø25	30	1/26	Kordina (1983)
19	Square	300	8.0	4Ø32	56	1	Myllymaki (1994)
20	Square	300	8.0	4Ø32	56	2	Myllymaki (1994)
21	Square	150	5.0	4Ø12	35	3	Myllymaki (1994)
22	Square	200	5.0	8Ø10	35	3	Renaud (2004)
23	Square	200	5.0	8Ø10	35	4	Renaud (2004)
24	Square	203	6.35	4Ø16	23	SQ-12	Chabot M (1992)
25	Square	254	6.35	4Ø16	23	SQ-18	Chabot M (1992)
26	Circular	273.1	6.35	4Ø20	23	C48	Chabot M (1992)
27	Circular	273.1	6.35	4Ø20	23	C49	Chabot M (1992)

Table III.1 Fire resistance of columns tested and calculated

Figure III-5 presents a comparison between calculated and measured temperatures in the column cross section of one particular test. Figure III-6 to Figure III-8 present in another way the same comparison for all the reference tests at the points indicated in Figure III-5.

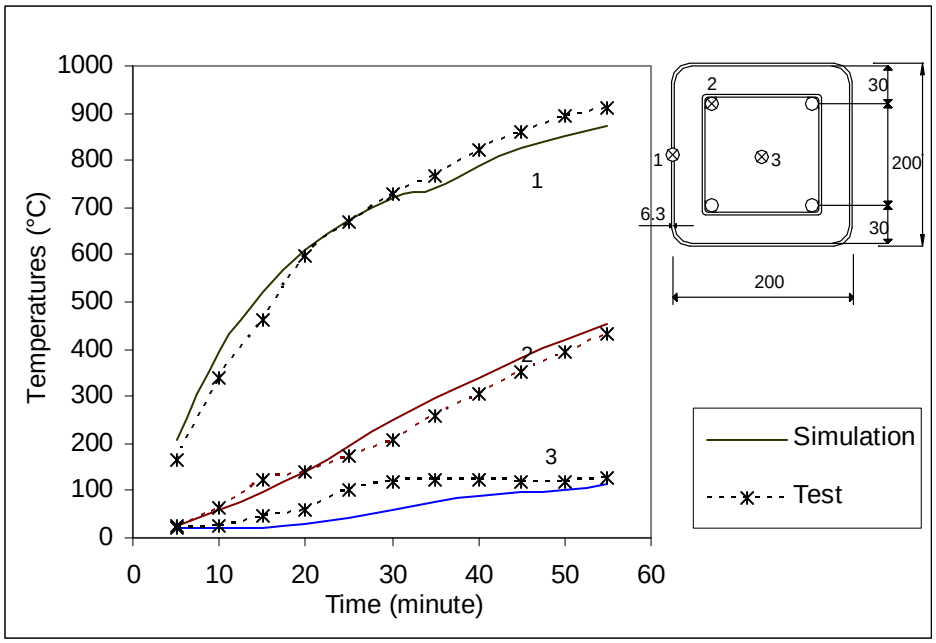

Figure III-5. Comparison between calculated and measured temperatures in the cross-section of one particular test

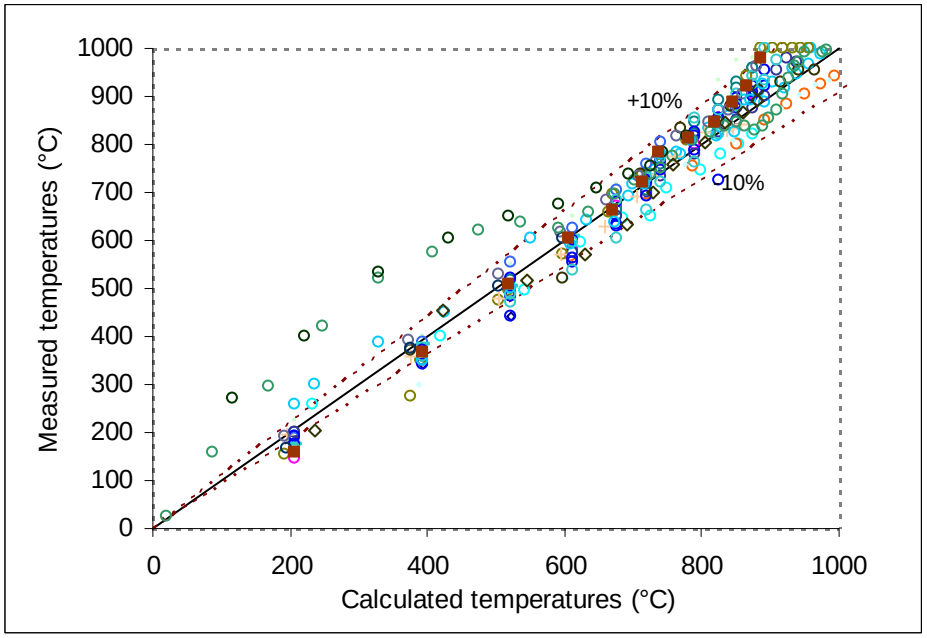

Figure III-6. Comparison between calculated and measured temperatures at steel surface of the reference tests

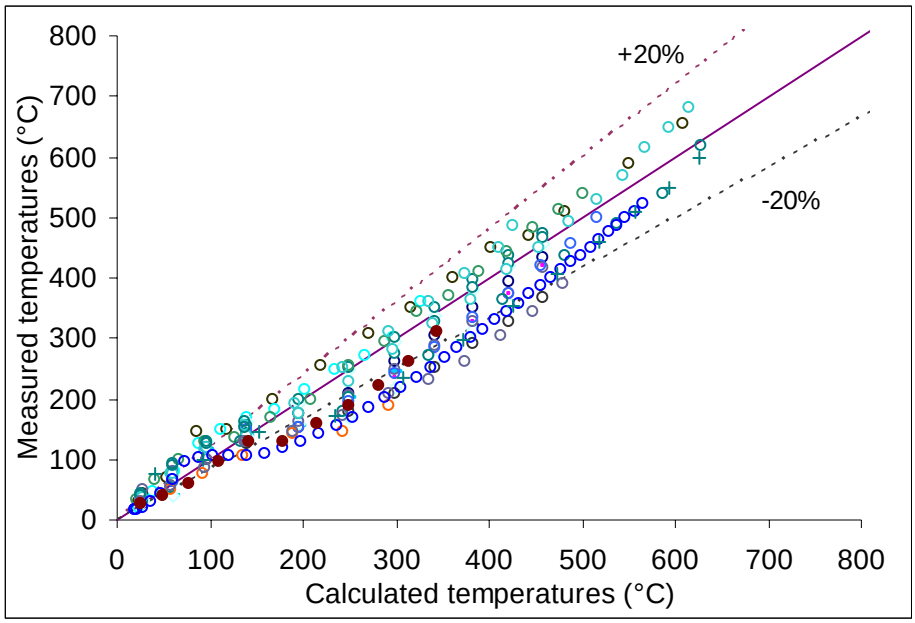

Figure III-7. Comparison between calculated and measured temperatures in the steel reinforcement of the reference tests

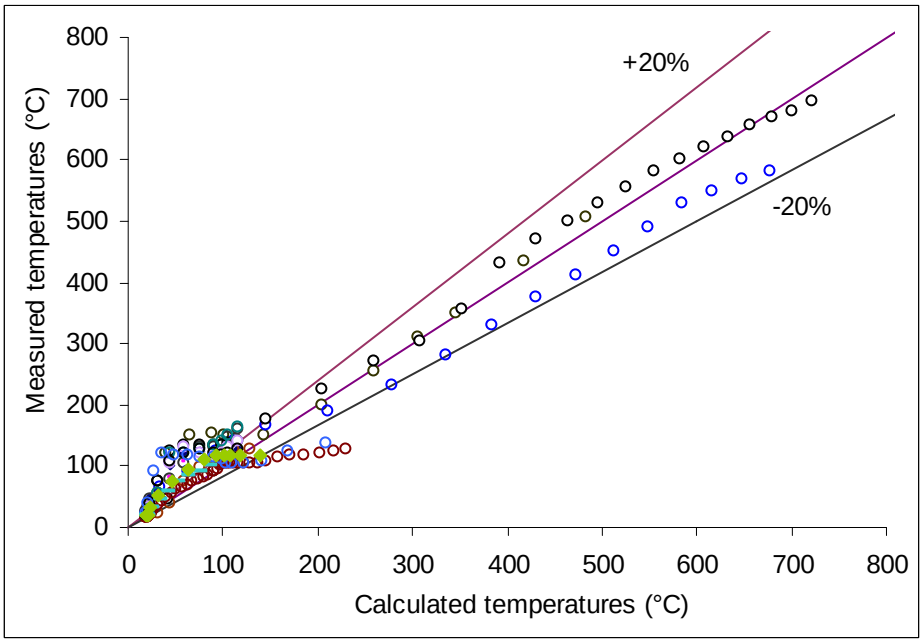

Figure III-8. Comparison between calculated and measured temperatures at the central point of the concrete core of the reference tests

The following comments can be drawn:

- Calculated temperatures on the hollow section are in good agreement with the measured temperatures provided thermal resistance defined previously is used in the calculation.
- Temperatures calculated in the longitudinal reinforcements are simulated satisfactorily but the differences between calculations and tests are more important than those found on the hollow steel section. These differences are explained on one hand by a certain uncertainty

of the real moisture content (fixed at 4% in calculations) and on the other hand by a water accumulation close to reinforcements subsequent to water migration (not taken into account in the model). In fact, part of this water moves to the external steel section, but can only escape through two holes generally drilled at the top and the bottom of the steel tube. This explains why the amount of vapour is more important than in classical reinforced concrete columns. Furthermore, another part of the vapour migrates toward the coldest zones where it condenses again, which results in a slowing down of the vaporisation phase.

- With regard to the point inside the concrete, the agreement is not so good especially at low temperatures. Once more the difference between theoretical and experimental curves is primarily the result of the length of the vaporisation stage. Differences between theoretical and experimental curves do not affect much the variation of material properties: for low temperatures, the concrete mechanical properties are not affected and for higher temperatures, the agreement between theory and experiment is good enough. On the contrary these differences influence the structural behaviour, as second order effects are produced by thermal gradients.

III.2.5 Conclusion

Calculations have been performed dealing with twenty seven column tests carried out in Europe and Canada. The simulations confirm that the temperatures calculated for steel hollow section filled with concrete are in agreement with reality provided a thermal resistance between the steel tube and the concrete core is introduced. The value adopted here is $0.013\ m^2K/W$. Of course, for some tests other (larger or smaller) values would have improved the correlation between the numerical and the experimental results, but as a whole, this value leads to the best correlation.

III.3 Structural model of SAFIR applied to CFSHS columns

III.3.1 The numerical approach for the structural analysis

A basis of for mechanical analysis of structures undergoing large displacements is the incremental form of the principle of virtual work. The formulation used in the model and the assembly of finite elements are based on the principle of virtual work expressed in a corotational description. In the model, a whole composite column is built up by means of several 2-D beam elements which are based on the following formulations and hypotheses:

- The large displacement type element is in a total corotational description;
- The displacement of the node line is described by the displacements of three nodes, two nodes at each end of the element supporting two translations and one rotation plus one node at mid-length supporting the non-linear part of the longitudinal displacement. The longitudinal displacement of the node line is a second-order power function of the longitudinal co-ordinate. The transversal displacement of the node line is a third-order power function of the longitudinal co-ordinate;

- Bernoulli's hypothesis is considered, i.e., the cross section remains plane under a bending moment;
- Von Karman's hypothesis is used: the strains are small;
- The rotations are assumed to be small (note that they are evaluated in the co-rotated configuration);
- The longitudinal integrations are numerically calculated using Gauss' method;
- The integration of the longitudinal stresses and stiffness on the section is based on the fibre model; the section is supposed to be made of a certain number of parallel fibres. In fact, the same discretisation as the one used for the thermal analysis is used. Each finite element of the thermal analysis, with its known material type and temperature, is considered as a fibre;
- The effect of thermal expansion of steel and concrete is considered in the constitutive models.

More information is given by Franssen J.M. (1997, 2005).

At the time this study started, the program SAFIR calculated the stress-strain relationship ($\sigma - \varepsilon$) of material at normal temperature by keeping the temperature of 20°C in the stress-strain relationship at elevated temperature. Because the concrete model of the fire part of Eurocode 2 has been derived independently from the model at room temperature, the $\sigma - \varepsilon$ relation for concrete used at normal temperature (according to EN 1992-1-1) is different from that for elevated temperatures (according to EN 1992-1-2) with a temperature of 20°C. We have introduced into the SAFIR code the new models CALCO_COLD and SILCO_COLD in order to model calcareous and siliceous concrete at room temperature respectively, like in EN 1992-1-1. The nonlinear stress-strain relations are indicated in Eurocode 2: EN 1992-1-1 (2004). The detail is shown in Appendix 1.

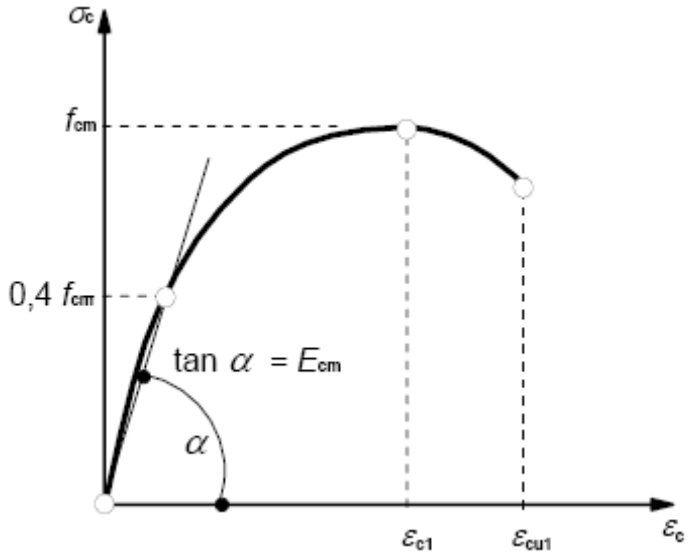

Figure III-9. Schematic representation of the stress- strain relation for structural analysis (EN 1992-1-1 (2004))

III.3.2 Main assumptions used in the numerical simulations

The following assumptions have been made for the numerical simulations of the structural behaviour of the columns:

- Each column is divided into 10 beam- elements;
- The geometric and material imperfections are taken into account by introducing an out-of-straightness of the columns. The initial deformation shape of the columns is regarded as a semi-sine curve. Five different values of the initial deflection at mid-height of the column are used to study the sensitivity of the fire resistance of the column to this parameter. As expected, the predicted fire resistance of CFSHS columns is higher when the initial displacement is smaller. However, the calculation results indicate that the effect of using a large range of different initial deflection values is relatively small. This inference is also supported by Ding J. and Wang Y.C (2008). In this study the initial deflection of L/500 has been used in simulations (tolerance given by EN 10210-2 for hot rolled structural hollow sections). It has always been considered that the effect of this eccentricity and the one of loading eccentricity are cumulative.
- In each column, there is no slip between the concrete core and the hollow steel section. Research studies by Renaud C. (2003a) and Ding J. *et al.* (2008) indicate that this assumption does not give a considerable error on the predicted fire resistance of columns.

III.3.3 Validity of the structural model

To examine the validity of the structural model, comparisons between simulated results and experiments have been done in two conditions: at room temperatures and in fire conditions.

III.3.3.1 Columns at room temperatures

A large number of experimental researches on the resistance of CFSHS columns under ordinary conditions have been performed (Shanmugam N.E. and Lakshmi B. (2001)). Only some tests on long columns with compact section (low D/t) have been chosen for comparison in order to eliminate confinement effects and local buckling of the steel wall.

The ultimate loads obtained from the tests (N_{test}) and calculated finite element analysis (N_{cal}) have been investigated. Table III.2 shows the results of all the reference tests. Some tests measure the compressive strength of concrete by cubic samples or cylinder sample 100mm * 200mm. The table gives the translated compressive strength of cylinder sample 150mm * 300mm. Some test results are extracted from the reference Roik K. and Bergmann R. (1989). The number of reference test “101 [24]” means the test N° 101 in reference 24 indicated in the report by Roik K. and Bergmann R. (1989).

Length	Section	Material strength (N/mm2)		Test load	eccentricity	Calculated load	Ncal/Ntest	Reference	
cm	mm*mm	Steel	concrete	N test(kN)	e (mm)	N cal (kN)		N°	Reference
231	C 121.0*5.68	344.2	21.1	786	3.55	625	0.80	101 [24]	Roik (1989)
231	C 121.0*5.49	343.2	21.1	816	1	663.75	0.81	102 [24]	Roik (1989)
167.64	C 152.7*3.15	415.1	20.9	881	_	875	0.99	12 [13]	Roik (1989)
436.5	C 218.3*6.05	302	32.6	1716	_	1672.5	0.97	1 [32]	Roik (1989)
328.5	C 218.3*6.45	302	30	2064	_	1927.5	0.93	2 [32]	Roik (1989)
194.7	C 101.7*2.4	410	53.65	361	10	333.75	0.92	SC-9	Kilpatrick (1999a)
194.7	C 101.7*2.4	410	53.65	309	15	292.5	0.95	SC-10	Kilpatrick (1999a)
321	R 120*80*5	386	37.4	600	_	620	1.03	1	Shakir-Khalil (1989)
321	R 120*80*5	386	34	393	24	373.75	0.95	2	Shakir-Khalil (1989)
400	R 120*80*6.3	370	55	368	55	294.5	0.80	RHS1	Wang Y.C. (1999a)
400	R 120*80*6.3	370	55	246	55	214.8	0.87	RHS2	Wang Y.C. (1999a)
320	R 120*80*6.3	370	55	520	55	539.62	1.04	RHS7	Wang Y.C. (1999a)
320	R 120*80*6.3	370	55	480	55	426.12	0.89	RHS8	Wang Y.C. (1999a)
260	R 150*100*4	495	60	1130	15	981.25	0.87	L1	Liu D. (2006)
260	R 150*100*4	495	60	884	30	780	0.88	L2	Liu D. (2006)
260	R 150*100*4	495	60	711	45	651.25	0.92	L3	Liu D. (2006)
260	R 150*100*4	495	60	617	60	562.5	0.91	L4	Liu D. (2006)
43.2	S 144*6.36	618	41.1	611	200	530.89	0.87	ER6_A_4_22	Fujimoto T. (2004)
43.2	S 144*6.36	618	41.1	1701	45	1452.17	0.85	ER6_A_4_61	Fujimoto T. (2004)
						average=	0.91		
						standard deviation =	0.07		

Table III.2 Load resistance of columns tested and calculated

It can be seen that a good agreement has been achieved for most of the columns.

III.3.3.2 Columns in fire

A comparison between the fire resistance of seventeen fire tests and corresponding calculation results has been performed. The seventeen fire tests considered here were carried out at the University of Braunschweig–Germany (Kordina K. and Klingsch W. (1983)) and in National Research Council of Canada (Chabot M. and Lie T.T. (1992), Mylymaki J. et al (1994)). Not all tests for the thermal validation have been chosen because in some of the preceding ones, not enough information was given in order to perform structural calculations.

The same test numbers are used in Table III.3 and Table III.1. The results of Table III.3 show that there is a good agreement between tests and numerical results.

Test Number	Section	Rebars	Length mm	Test loading		Measured failure time Rtest (min)	Calculated failure time Rcal (min)	Rcal/Rtest
				Load (kN)	e (mm)			
1	200*6.3	4Ø18	4200	432	20	63	50.8	0.81
2	200*6.3	4Ø18	4200	318	50	58	53.8	0.93
3	200*6.3	4Ø18	4200	537	5	61	48.1	0.79
4	200*6.3	4Ø18	4200	213	100	79	60.4	0.76
5	260*7.1	4Ø18	4200	1237	26	37	49.6	1.34
6	300*7.0	4Ø18	4200	1000	30	90	89.2	0.99
7	200*6.3	4Ø18	3700	649	20	39	47.8	1.23
8	200*6.3	4Ø10	4200	551	20	23	24	1.04
10	200*6.3	4Ø18	3700	649	20	56	52.9	0.94
12	200*6.3	4Ø18	4200	550	5	59	51.4	0.87
13	200*6.3	4Ø18	3700	294	20	82	66.3	0.81
15	220*6.3	4Ø18	4200	375	22	68	60.5	0.89
16	220*6.3	6Ø20	4200	421	22	88	83.6	0.95
17	260*7.1	6Ø22	4200	869	26	64	75.3	1.18
18	300*7.0	6Ø25	4200	1507	30	56	70.1	1.25
24	203*6.35	4Ø16	3810	500	0	150	84	0.56
25	254*6.35	4Ø16	3810	1440	0	113	82	0.73
							Rmean=	0.95
							standard deviation=	0.201

Table III.3 Fire resistance of columns tested and calculated

III.3.4 Conclusion

The model can simulate in a suitable way the structural behaviour of CFSHS columns and provides a good estimation of the fire resistance due to the choice of appropriate material laws as well as introduction initial out-of-straightness. The model can thus be used to study parametrically the behaviour of CFSHS columns under both ordinary and fire conditions.

CHAPTER IV: ULTIMATE LOAD OF SELF_COMPACTING CONCRETE FILLED HOLLOW STEEL COLUMNS AT NORMAL TEMPERATURE

IV.1 The method of EC 4: EN 1994-1-1 for CFSHS columns

IV.1.1 Method of the current European standard EN 1994-1-1 (2004)

In the field of columns and compression members EC4 can be applied to members with steel grades S235 to S460 and normal weight concrete of strength classes C20/25 to C50/60. The scope of the simplified method has some limitations:

- The steel contribution ratio δ should fulfil the following condition: $0.2 \le \delta \le 0.9$

  where $\delta = \dfrac{A_a f_{yd}}{N_{Pl,Rd}}$, $N_{pl,Rd}$ is the plastic resistance to compression of the section:

$$N_{pl,Rd} = A_a.f_{yd} + A_c.f_{cd} + A_s.f_{sd}$$

  where A_a , A_c , A_s are the area of the steel hollow section, the concrete section and the reinforcement, respectively; f_{yd} , f_{cd} , f_{sd} are the design strength of the steel hollow section, the concrete section and the reinforcement, respectively.

- Only members of doubly symmetrical and uniform cross-section over the member length can be considered.
- The longitudinal reinforcement that may be used in calculation should not exceed 6% of the concrete area.
- The relative slenderness $\overline{\lambda}$ should fulfil the condition $\overline{\lambda} \le 2.0$.
- The relative slenderness $\overline{\lambda}$ for the plane of bending being considered is given by:

$$\overline{\lambda} = \sqrt{\frac{N_{pl,Rk}}{N_{cr}}} \qquad \text{(IV.1)}$$

  where:

  $N_{pl,Rk}$ the characteristic value of the plastic resistance to compression given by

$$N_{pl,Rk} = A_a.f_y + A_c.f_{ck} + A_s.f_{sk}$$

  f_y , f_{ck} , f_{sk} are the characteristic strength of the steel hollow section, the concrete section and the reinforcement, respectively

  N_{cr} is the elastic buckling load of the column

$$N_{cr} = \frac{(EI)_{eff}\pi^2}{L^2} \qquad \text{(IV.2)}$$

  L is the effective length of the column

$$(EI)_{eff} = E_a.I_a + K_e.E_{cm}.I_c + E_s I_s$$

  K_e is a correction factor that should be taken as 0.6

E_a, E_s are the respective elastic modulus of the steel of the structural section and of the reinforcement;

E_{cm} is the elastic secant modulus of the concrete

I_a, I_c, I_s are the second moments of area of the structural steel section, the un-cracked concrete section and the reinforcement for the bending plane being considered.

The procedure for calculating the ultimate load of a CFSHS column with the above-mentioned scope is:

Step 1: Calculation of the plastic resistance to compression $N_{pl,Rd}$ of the section:

$$N_{pl,Rd} = A_a f_{yd} + A_c f_{cd} + A_s f_{sd} \quad \text{(IV.3)}$$

For concrete filled tubes of circular cross-section, account may be taken of the increase in strength of concrete caused by confinement provided that the relative slenderness $\bar{\lambda}$ does not exceed 0.5 and e/d <0.1, where *e* is the eccentricity of loading and *d* is the external diameter of the column. The plastic resistance to compression may then be calculated from the following expression:

$$N_{pl,Rd} = \eta_a A_a f_{yd} + A_c f_{cd}(1 + \eta_c \frac{t}{d}\frac{f_y}{f_{ck}}) + A_s f_{sd} \quad \text{(IV.4)}$$

where t is the wall thickness of the steel tube.

For members with e=0, the value $\eta_a = \eta_{ao}$ and $\eta_c = \eta_{co}$ are given by following expressions:

$$\eta_{ao} = 0.25(3 + 2\bar{\lambda}) \text{ (but } \le 1.0) \quad \text{(IV.5)}$$

$$\eta_{co} = 4.9 - 18.5\bar{\lambda} + 17\bar{\lambda}^2 \text{ (but } \ge 0) \quad \text{(IV.6)}$$

For members in combined compression and bending with 0<e/d<0.1, the values η_a and η_c should be determined from (IV.7) and (IV.8) where η_{ao} and η_{co} (IV.5) and (IV.6)

$$\eta_a = \eta_{ao} + (1 - \eta_{ao})(10e/d) \quad \text{(IV.7)}$$

$$\eta_c = \eta_{co} + (1 - 10e/d) \quad \text{(IV.8)}$$

For e/d >0.1, $\eta_a = 1.0$ and $\eta_c = 0$.

Step 2: Calculating the resistance of members in axial compression adopted the European buckling curves

$$N_{Rd} = \chi N_{pl,Rd} \quad \text{(IV.9)}$$

where χ is reduction factor for flexural buckling obtained from the relative slenderness $\bar{\lambda}$ and the relevant buckling curve:

$$\chi = \frac{1}{\Phi + \sqrt{\Phi^2 - \bar{\lambda}^2}} \qquad \text{(IV.10)}$$

$$\text{with } \Phi = 0,5[1 + \alpha(\bar{\lambda} - 0,2) + \bar{\lambda}^2] \qquad \text{(IV.11)}$$

α is an imperfection factor α =0.13 for curve "a_0"
α =0.21 for curve "a"
α =0.34 for curve "b"
α =0.49 for curve "c"
α =0.76 for curve "d"

For circular and rectangular hollow steel section with the reinforcement ratio ($\rho_s = A_s / A_c$) $\rho_s \le 3\%$, buckling curve "a" is applied, and with $3\% \le \rho_s \le 6\%$ buckling curve "b" is applied. For circular hollow steel sections with an internal I-section, buckling curve "b" is also applied.

Step 3: In the case of axial forces and additional bending moment, an interaction curve for combined compression and bending of the cross-section is determined (the continuous line in Figure IV-1). It may be calculated assuming rectangular stress block, taking into account the design shear force if the shear force on the steel section exceeds 50% of the design shear resistance of the steel section. The tension strength of the concrete should be neglected. As a simplification, the interaction curve may be replaced by a polygonal diagram (the dashed line in Figure IV-1). Figure IV-2 shows an example of the plastic stress distribution of a concrete filled hollow section.

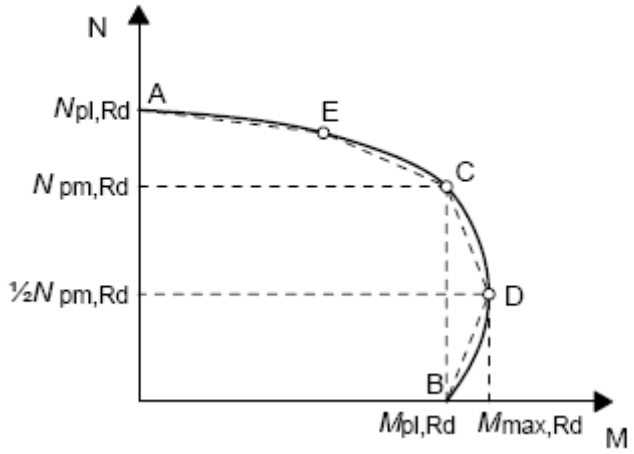

Figure IV-1. Interaction curve for combined compression and uniaxial bending

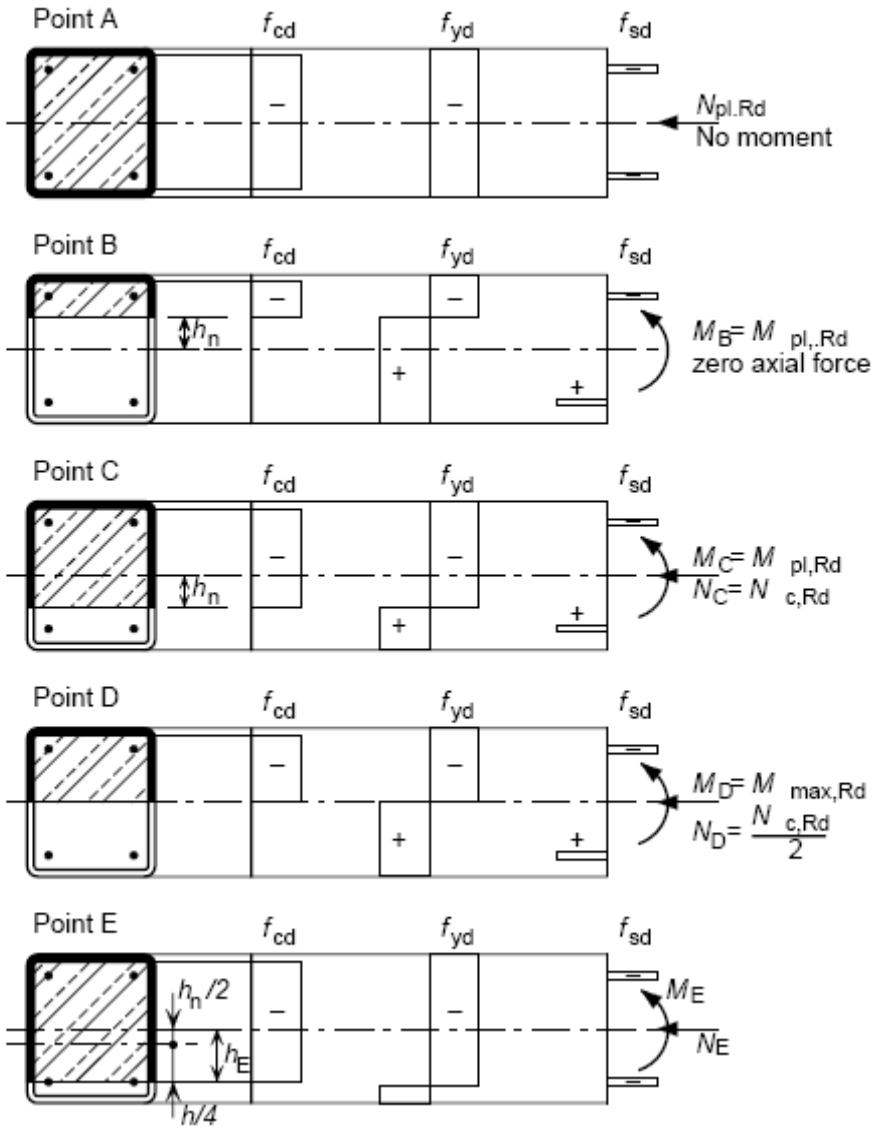

Figure IV-2. Stress distributions for the points of the interaction curve for concrete filled hollow sections

IV.1.2 Considerations on the European buckling curves

According to the method of EC4 described above, the ultimate design compressive load is determined using the European buckling curves:

$$N_{Rd} = \chi N_{pl,Rd} \tag{IV.12}$$

with χ being a reduction factor according to EC3 dependant on the relative slenderness $\bar{\lambda}$ and the respective buckling curve. The curves are the result of an international experimental and theoretical investigation, performed under the authority of the European Convention for Construction Steelwork (E.C.C.S), of the strength of steel columns considering the influence of type of cross section and manufacture procedures. More than 1000 buckling tests, on various types of members (I, H, T, U, circular and square hollow sections), with different values of slenderness (between 55 and 160) were studied (ECCS (1976)). A probabilistic

approach, using the experimental strength, associated with a theoretical analysis, showed that it was possible to draw some curves describing column strength as a function of the reference slenderness. The imperfections which have been taken into account are: a half sine-wave geometric imperfection of magnitude equal to 1/1000 of the length of the column; and the effect of residual stresses relative to each kind of cross-section. The works have led to the proposal of a set of five buckling curves (Figure IV-3) in tabular or graphical form (ECCS (1978)).

However, the tabular or graphical presentation of these buckling curves is not well adapted to the modern tools used for the design of structures. Indeed, computers require analytical expressions. Based on Ayrton-Perry expression, Rondal J. and Maquoi R. (1981) have proposed the buckling of steel columns- an equation giving, with an excellent accuracy, the same results as the tables recommended by E.C.C.S. This relation has been adopted by E.C.C.S, Eurocodes and numerous national specifications. These five curves reflect the differences in imperfections including geometric imperfections (lack of verticality, lack of straightness, lack of flatness, accidental eccentricity of loading) and mechanical imperfection (residual stresses and variations of the yield stress). Such imperfections result in bending moments developing at an early stage of loading in essentially axially loaded columns, and the failure load of a real steel columns thus be seen to depend not only on its slenderness ratio but also on the mechanical properties of its material.

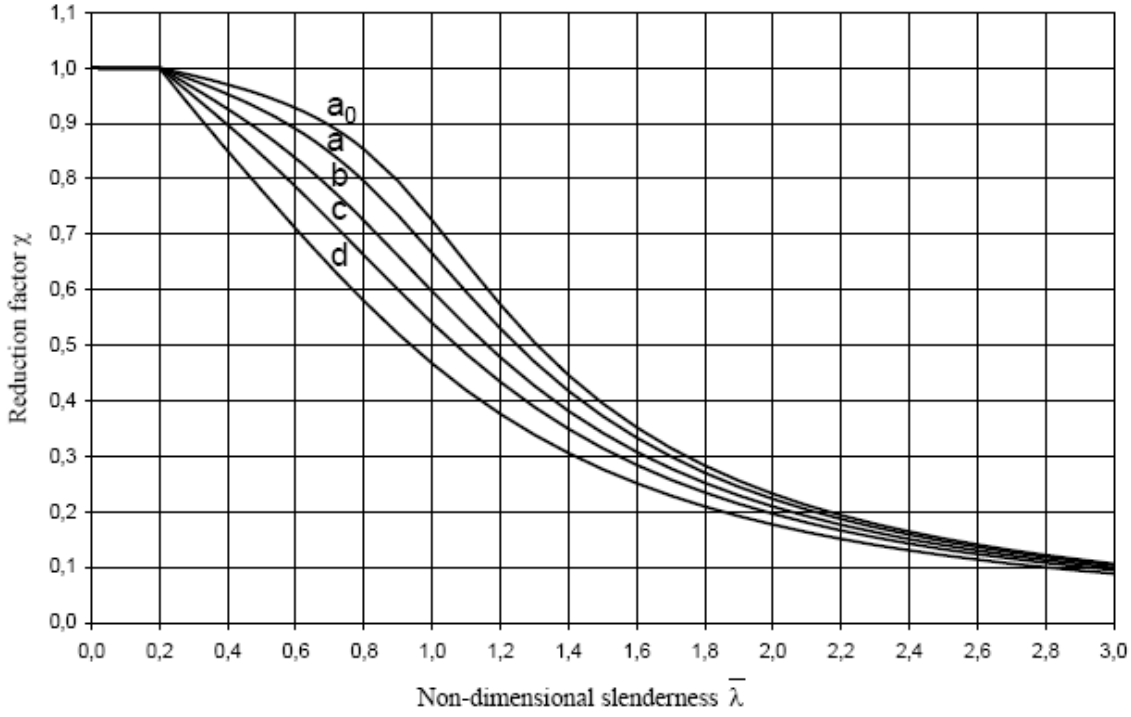

Figure IV-3. Buckling curves (EN 1993-1-1)

Virdi K.S. and Dowling P.J (1976) are the first researchers applied the European buckling curves (built for steel struts) to composite columns by define the slenderness in the case of column comprised of more than one material.

Roik K. *et al.* determined the axial compression resistance of composite columns by the help of the European strut curves. The ultimate strength analysis of composite compression member with imperfection has been carried out by means of a computer program derived at Bochum University (Roik K. *et al.* (1977)). For simplification, this numerical model assumed only representative geometrical imperfections to take into account both geometrical imperfection and material inhomogenities. Many load carrying capacities of available tests have been examined and showed good agreements. In the reference Roik K. and Bergmann R. (1989), tests on quite slender composite columns showed that European strut curves represent satisfactorily their failure load. However, there are two major problems which result from this approach. First, the imperfection parameter set for steel columns must be changed to an appropriate value for composite columns, but this can be achieved through an analysis of available test results. The second is in the definition of the column slenderness. This is because the effective stiffness must be calculated for different materials: structural steel, concrete, and reinforced steel. These problems are solved to give the design method indicated in Eurocode 4.

In preliminary version of European code ENV 1994-1-1 (1992), buckling curve "*a*" is used for concrete filled tube columns with effective flexural stiffness $(EI)_{eff} = E_a.I_a + 0.8.\frac{E_{cm}}{\gamma_c}.I_c + E_s I_s$ where the material safety factor γ_c can be reduced to γ_c = 1.35 for the determination of the effective bending stiffness, according to Eurocode 2.

In current version of Eurocodes EN 1994-1-1 (2004), circular or rectangular hollow section columns filled with plain concrete or containing up to 3% reinforcement can be designed using buckling curve "*a*". Concrete filled sections containing from 3% to 6% reinforcement must be designed using buckling curve "*b*". In addition, concrete filled circular hollow section columns containing an internal I-section can also be designed using buckling curve "*b*". The effective flexural stiffness is $(EI)_{eff} = E_a.I_a + 0.6.E_{cm}.I_c + E_s I_s$. The 0.6 factor is an empirical multiplier, which has been determined from calibration, to give good agreement with test results (Corus Tubes (2002)).

Because the limit of application in EC4 is the longitudinal reinforcement ratio less than 6%, the question that arises is which buckling curve is relevant for columns with a high percentage of reinforcement (exceeding 6%) and other types of hollow steel sections filled with concrete and containing an internal steel profile (Figure IV-4).

Numerical investigation has been realised for CFSHS columns of existing range (reinforcement from 3% to 6% of reinforcement and circular containing addition I-section) and extended range (reinforcement from 6% to 10% and other types of steel sections filled with concrete and containing an internal steel profile). It is assumed that geometric imperfections are the same for the existing and the extended range. The effect of residual stresses on the load resistance of columns with bar reinforcements does not depend on the reinforcement ratio but in case of an internal steel profile (Figure IV-4), this effect depends on the type of profile. Nevertheless, for columns axially loaded without local buckling, the

residual stresses have little influence. Thus we assume the same initial deformation of the columns for both existing range and extended range to account for the collective effects of all geometric imperfections and residual stresses. Comparison between buckling curves of the two ranges can give an indication of the buckling curves to be adopted for the extended range of CFSHS columns.

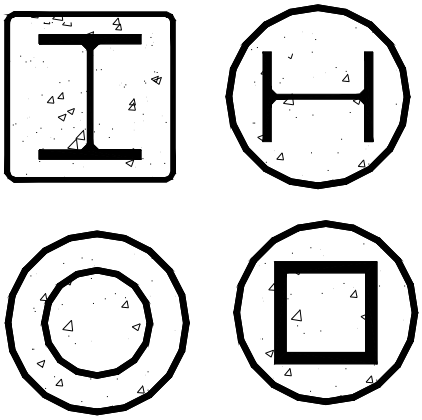

Figure IV-4. CFSHS section with an embedded steel profile

IV.2 The buckling curve for CFSHS columns with dense reinforcements

IV.2.1 Assumptions for numerical simulations

Assumptions for numerical simulations have described in part III.3.2. The analysis of axially loaded columns is based on a shape with an initial lateral bow. Equivalent bow imperfections are to be used, to represent residual stresses in the steel section, as well as geometric imperfections. The initial deformation shape of the columns is regarded as a semi-sine curve with maximum deflection at middle height of L/500. Numerical buckling loads of columns with existing range of reinforcement (from 3% to 6%) corresponding to buckling curve “b” indicate that choosing a member imperfection L/500 for non-linear second-order analysis of CFSHS columns is relevant.

Numerical simulations have been performed with various cross section dimensions (from 150mm to 300mm), reinforced steel ratios (from 3% to 10%), concrete strengths (C30, C40 and C50) and concrete covers (from 30mm to 45mm).

IV.2.2 Simulations results

Results show that the buckling mode of CFSHS columns with a high percentage of reinforcement or with an embedded steel profile is still close to the results given by curve “b”. Some cases are shown from Figure IV-6 to Figure IV-18.

Figure IV-5 shows the buckling curves of columns with various percentages of reinforcement. It can be seen that for sections with low reinforcement ratio (from 0% to 3%) the buckling curves are near curve “a” as suggested in EC4 and with a reinforcement ratio from 3% to 6% near curve “b”. For columns with dense reinforcement (above 6%) the buckling curves are near curve “b” also. The ultimate load of short columns (low relative slenderness) obtained from numerical simulations are lower than the value calculated using buckling curves because

confinement effects are ignored in simulation while buckling curve obtained from available test results show confinement effects.

The following symbols have been used in the figures:

S200-6.3 stands for Square section with dimension D=200 mm, steel wall thickness t =6.3 mm

C40 stands for characteristic compression strength of concrete on cylinder f_{ck} = 40 MPa

Dr45 stands for concrete cover Dr = 45 mm

12D18 stands for the case: reinforcement in the section consists of 12 bars with diameter 18mm.

As = 1.7% stands for the reinforcement ratio of the section is $A_s / A_c = 1.7\%$

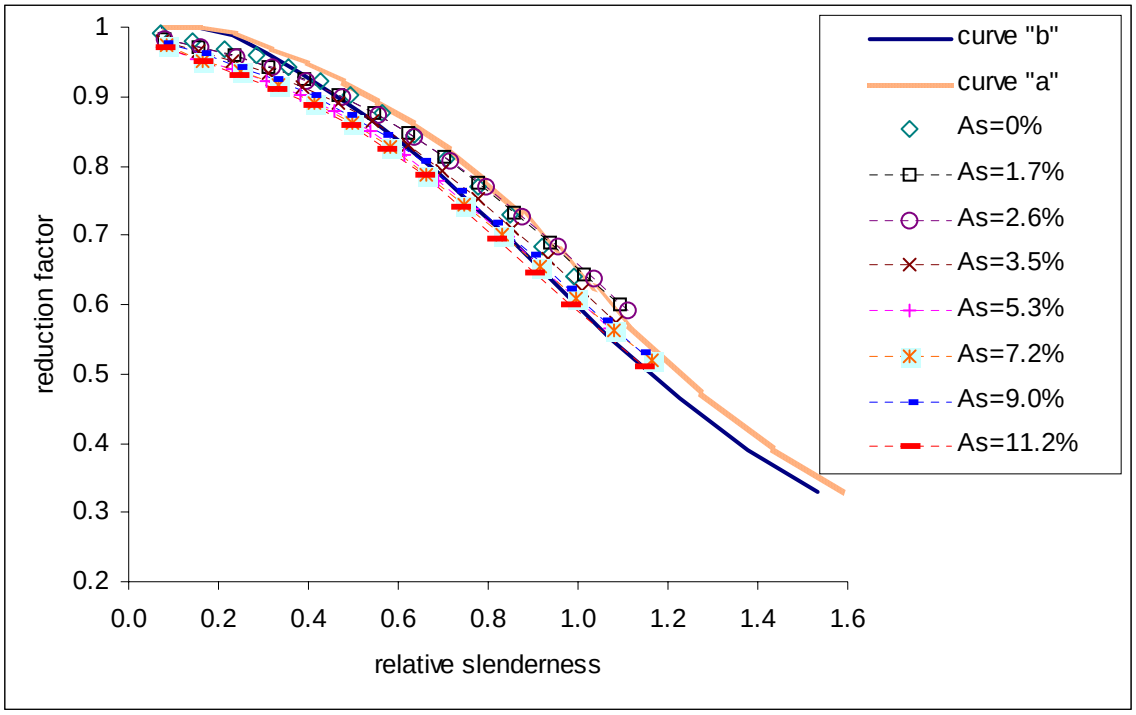

Figure IV-5. Buckling curve of column with square section S260_8

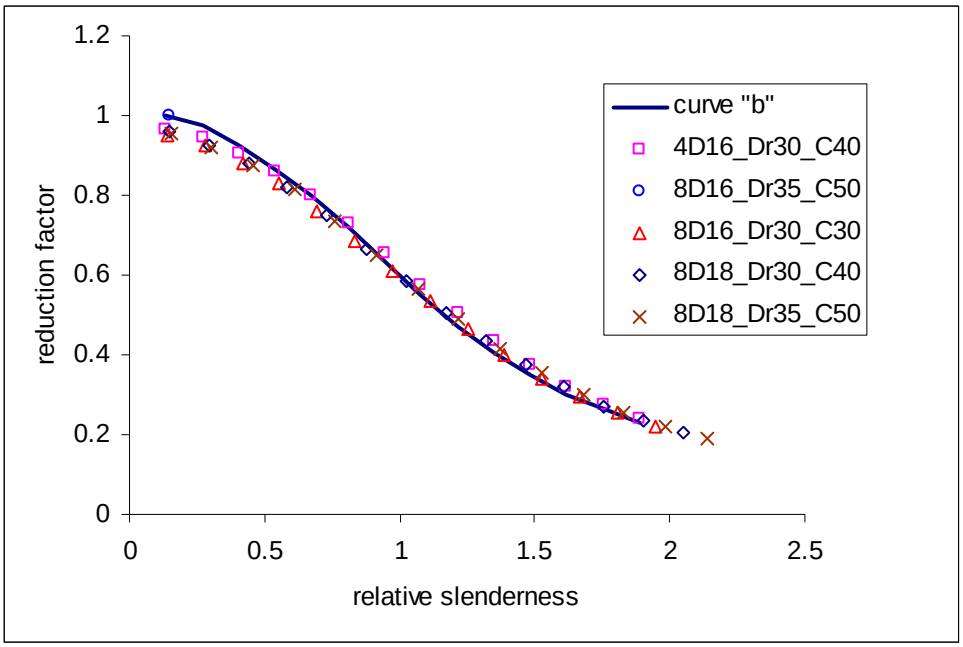

Figure IV-6. Buckling curve of column with square section S150_5

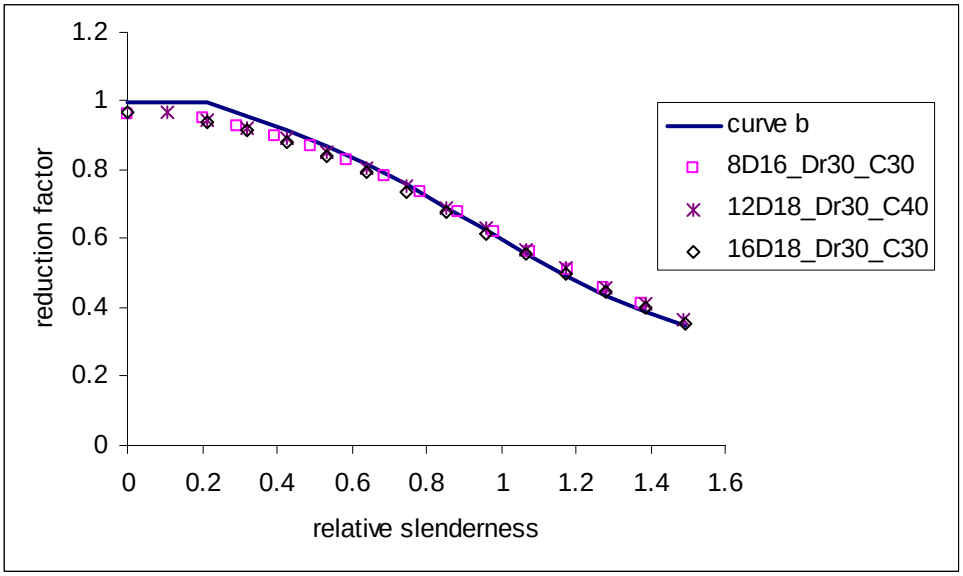

Figure IV-7. Buckling curve of column with square section S200_6.3

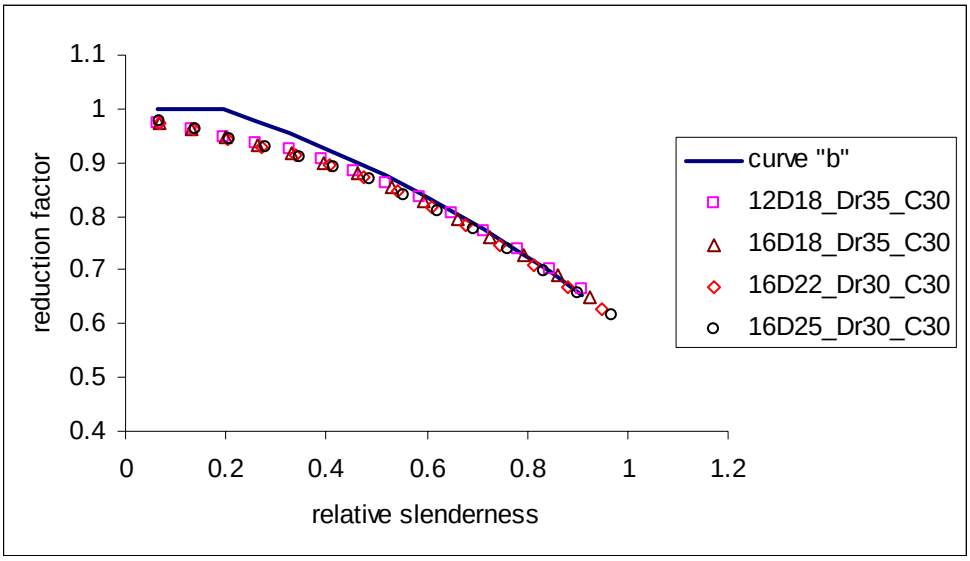

Figure IV-8. Buckling curve of column with square section S300_8

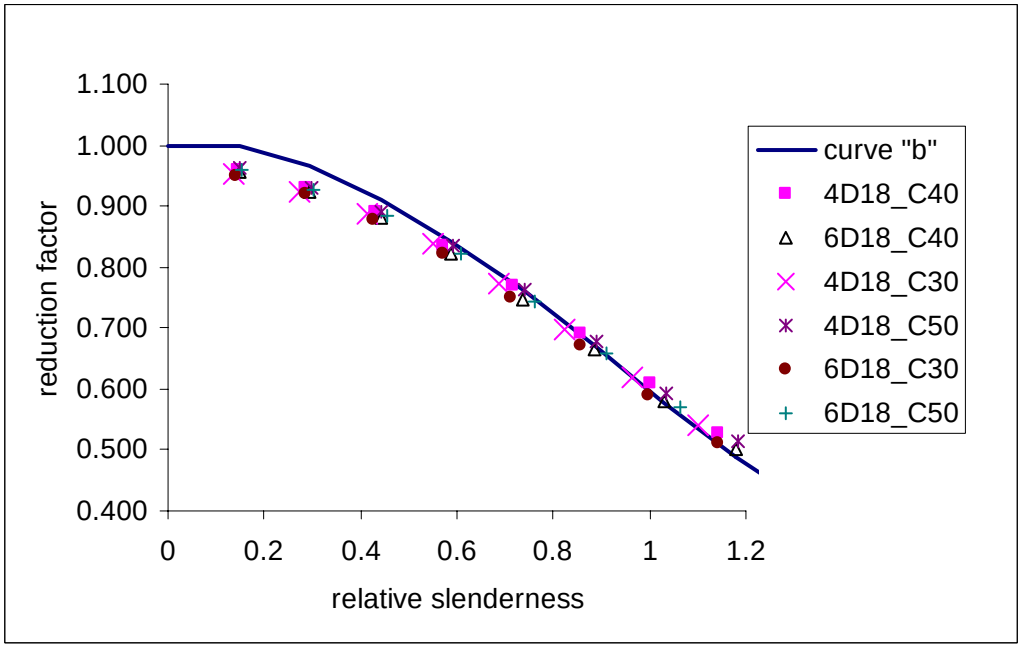

Figure IV-9. Buckling curve of column with circular section C168.3_5

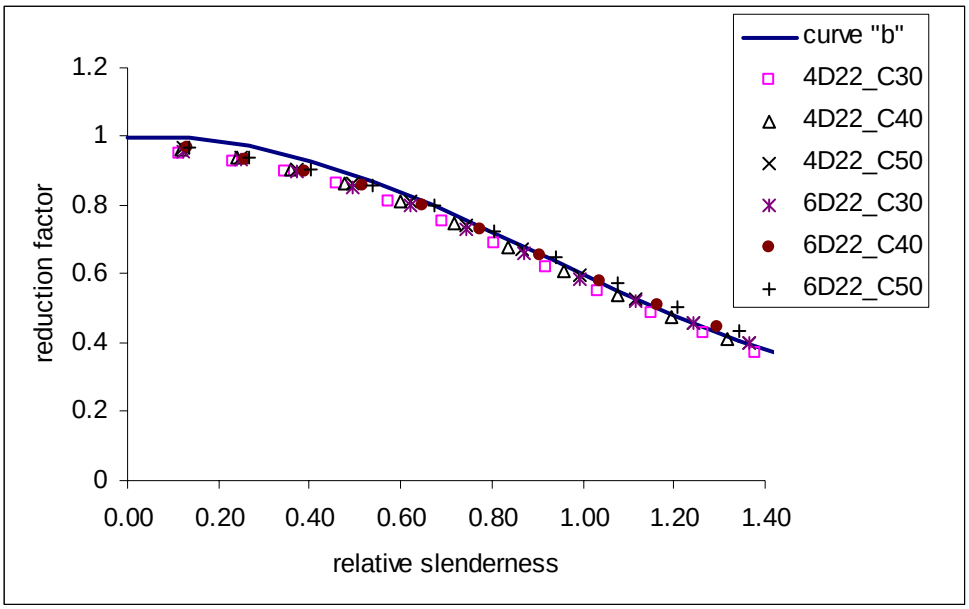

Figure IV-10. Buckling curve of column with circular section C197.3_5

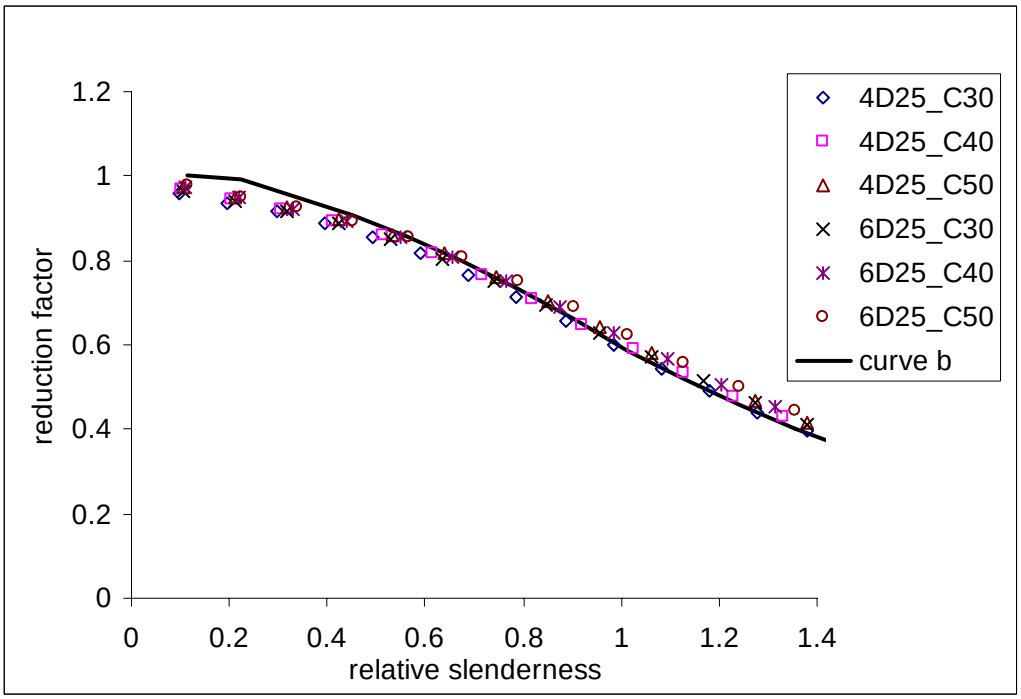

Figure IV-11. Buckling curve of column with circular section C244.5_5

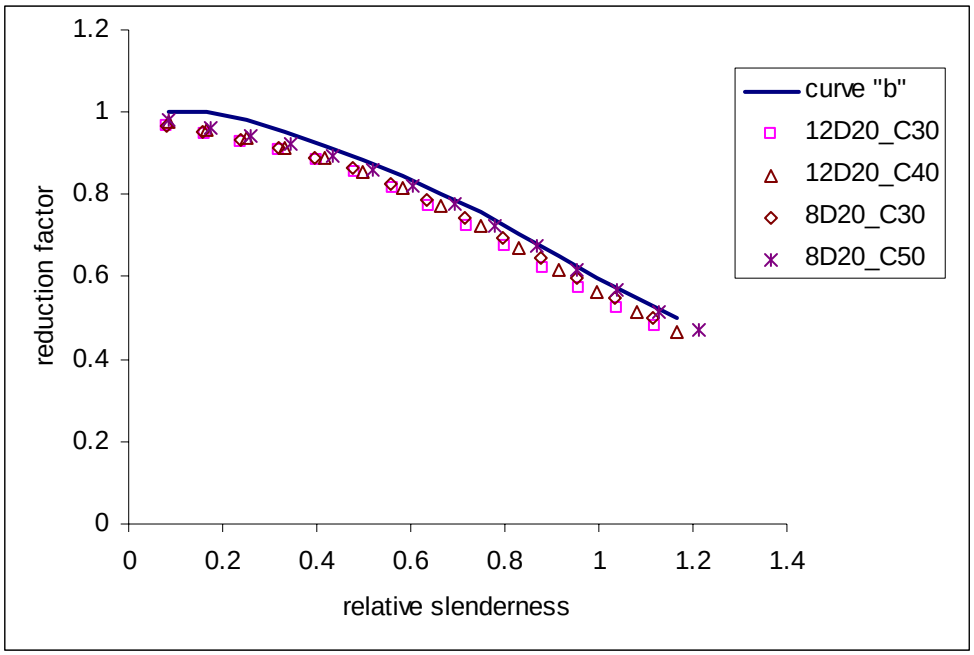

Figure IV-12. Buckling curve of column with circular section C273_6.35

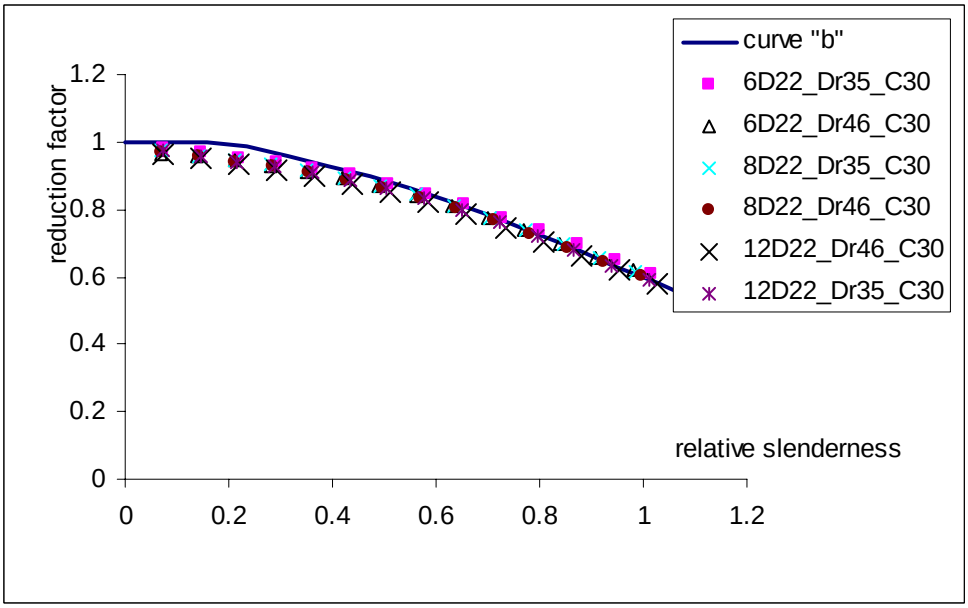

Figure IV-13. Buckling curve of column with circular section C323.9_8

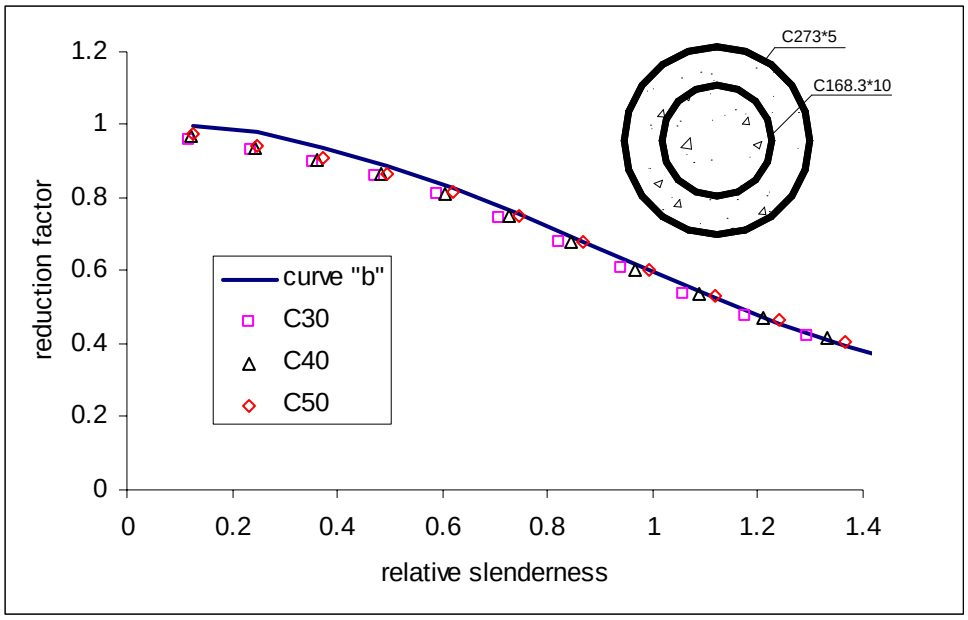

Figure IV-14. Buckling curve of column with double tubes

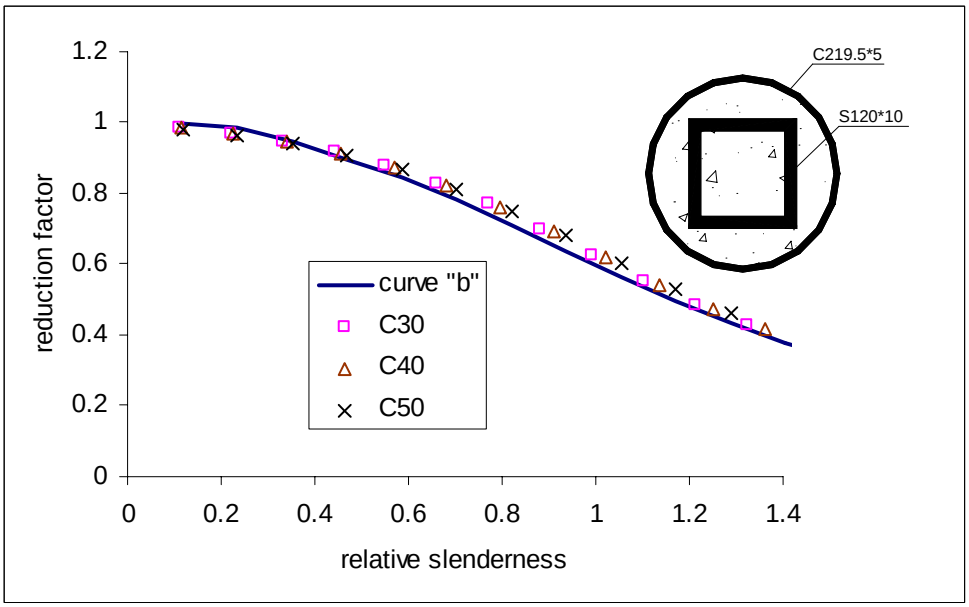

Figure IV-15. Buckling curve of column with double tubes

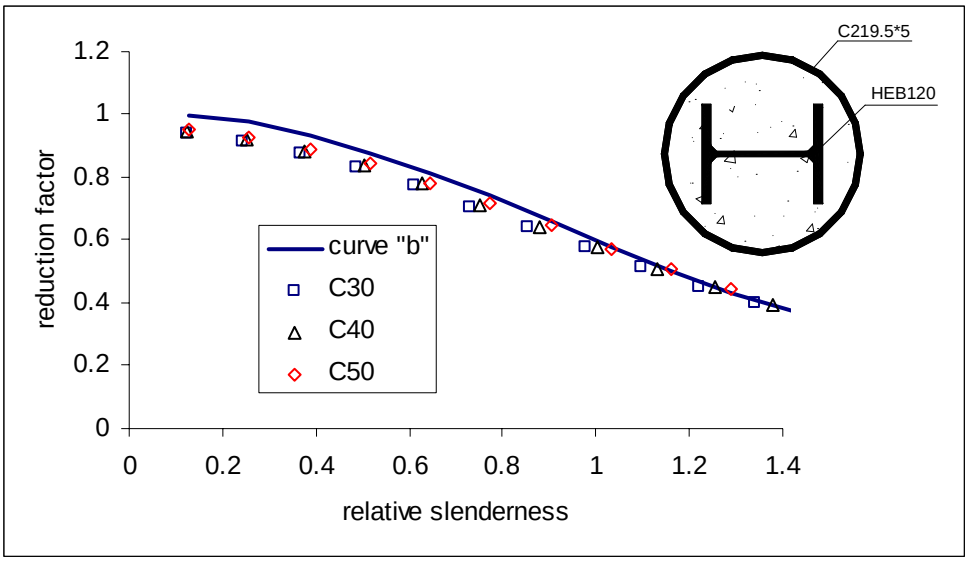

Figure IV-16. Buckling curve of circular column with internal I profile

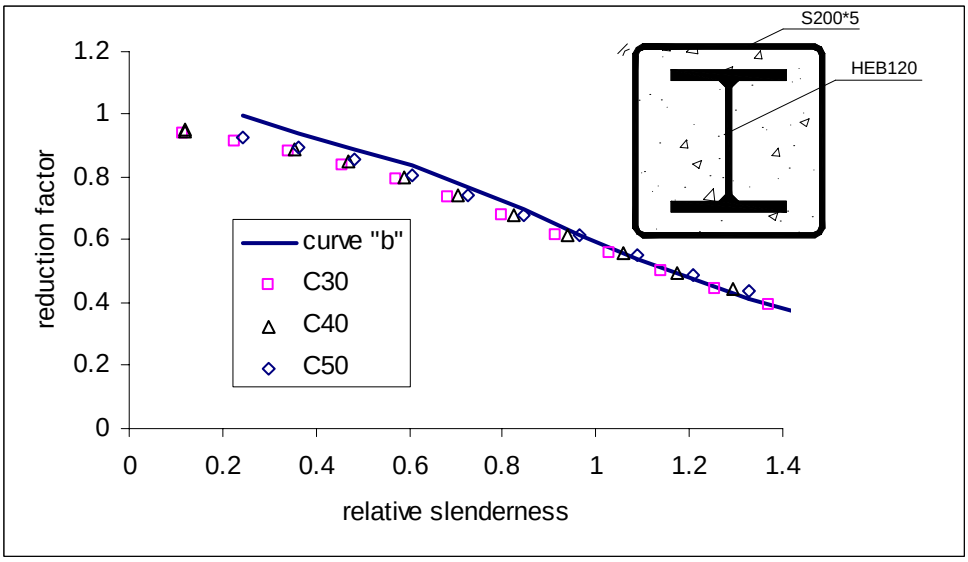

Figure IV-17. Buckling curve of square column with internal I profile

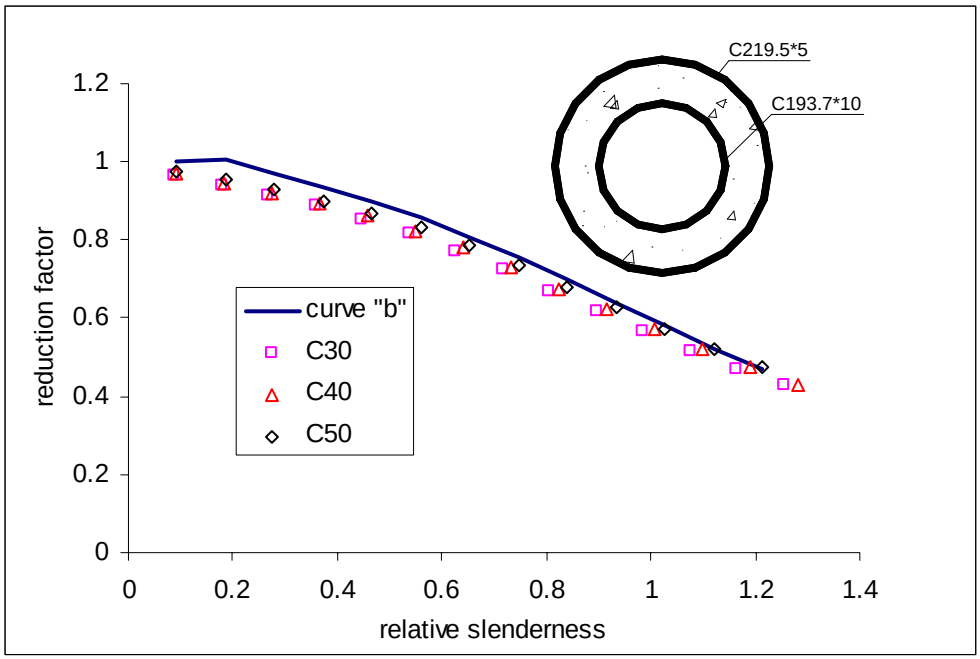

Figure IV-18. Buckling curve of column with double tubes

IV.2.3 Conclusions

Results from numerical simulations with various cross section dimensions, reinforced steel ratios, concrete strengths and concrete covers show that:

- The buckling curves for CFSHS columns with dense steel bar reinforcement (from 6% to 10%) are the same as the buckling curves for CFSHS columns with steel bar reinforcement from 3% to 6%. In current version of Eurocode EN 1994-1-1 (2004), circular or rectangular hollow section columns filled with concrete containing from 3% to 6% reinforcement must be designed using buckling curve "*b*". This means that CFSHS columns with dense steel bar reinforcement have to be designed using buckling curve "*b*" also;

- The buckling curves for CFSHS columns with an embedded steel profile (Figure IV-4) are the same as the buckling curves for concrete filled circular hollow section columns containing an embedded I-section. This type of columns has to be designed using buckling curve "*b*" according to EN 1994-1-1 (2004).